

Free Antineutrino Absorption Cross Section. I. Measurement of the Free Antineutrino Absorption Cross Section by Protons*

FREDERICK REINES AND CLYDE L. COWAN, JR.†

Los Alamos Scientific Laboratory, University of California, Los Alamos, New Mexico

(Received September 8, 1958)

The cross section for the reaction $p(\bar{\nu},\beta^+)n$ was measured using antineutrinos ($\bar{\nu}$) from a powerful fission reactor at the Savannah River Plant of the United States Atomic Energy Commission. Target protons were provided by a 1.4×10^3 liter liquid scintillation detector in which the scintillator solution (triethylbenzene, terphenyl, and POPOP) was loaded with a cadmium compound (cadmium octoate) to allow the detection of the reaction by means of the delayed coincidence technique. The first pulse of the pair was caused by the slowing down and annihilation of the positron (β^+), the second by the capture of the neutron (n) in cadmium following its moderation by the scintillator protons. A second giant scintillation detector without cadmium loading was used above the first to provide an anticoincidence signal against events induced by cosmic rays. The antineutrino signal was related to the reactor by means of runs taken while the reactor was on and off. Reactor radiations other than antineutrinos were ruled out as the cause of the signal by a differential shielding experiment. The signal rate was 36 ± 4 events/hr and the signal-to-noise ratio was $\frac{1}{5}$, where half the noise was correlated and cosmic-ray associated and about half was due to non-reactor-associated accidental coincidences. The cross section per fission $\bar{\nu}$ (assuming 6.1 $\bar{\nu}$ per fission) for the inverse beta decay of the proton was measured to be $(11 \pm 2.6) \times 10^{-44}$ cm²/ $\bar{\nu}$ or $(6.7 \pm 1.5) \times 10^{-43}$ cm²/fission. These values are consistent with prediction based on the two-component theory of the neutrino.

I. INTRODUCTION

A DETERMINATION of the cross section for the reaction: antineutrino ($\bar{\nu}$) on a proton (p^+) to yield a positron (β^+) and a neutron (n),



permits a check to be made on the combination of fundamental parameters on which the cross section depends. Implicit in a theoretical prediction of the cross section are (1) the principle of microscopic reversibility, (2) the spin of the $\bar{\nu}$, (3) the particular neutrino theory employed: e.g., two- or four-component, (4) the neutron half-life and its decay electron spectrum, and (5) the spectrum of the incident $\bar{\nu}$'s.

An experiment which was performed to identify antineutrinos from a fission reactor¹ yielded an approximate value for this cross section. Following this work, however (and prior to the parity developments involved in point 3), the equipment was modified in order to obtain a better value of the cross section. The modification consisted in the addition of a cadmium salt of 2-ethylhexanoic acid to the scintillator solution² of one of the detectors of reference 1, utilizing the protons of the solution as targets for antineutrinos, and making the necessary changes in circuitry to observe both positrons and neutron captures in the detector resulting from antineutrino-induced beta decay in the detector. In addition, a second detector used in the experiment

of reference 1 was now used as an anticoincidence shield against cosmic-ray-induced backgrounds, and static shielding was increased by provision of a water tank about 12-inches thick below the target detector. The delayed-coincidence count rate resulting from the positron pulse followed by the capture of the neutron was observed as a function of reactor power, and an analysis of the reactor-associated signal yielded, in addition to an independent identification of the free antineutrino, a measure of the cross section for the reaction and a spectrum of first-pulse (or $\bar{\nu}$) energies. Since the antineutrino spectrum is simply related to the β^+ spectrum, the measurement yields an antineutrino spectrum above the 1.8-Mev reaction threshold. The spectrum is, however, seriously degraded by edge effects in the detector.

This experiment was identical in principle with that performed at Hanford in 1953.³ It was, however, definitive from the point of view of antineutrino identification (whereas the Hanford experiment was not) because of a series of technical improvements, coupled with the better shielding against cosmic rays achieved by going underground. The improvements consisted in the use of an isolated power supply to diminish electrical noise from nearby machinery, better shielding from the reactor gamma-ray and neutron background, a more complete anticoincidence shield against charged cosmic rays through the use of a liquid scintillation detector, and use of a large detector containing 6.5 times as many proton targets.⁴ In addition, oscilloscopic presentation and photographic recording of the data assisted materially in analyzing the signals and rejecting electrical noise.

* Work performed under the auspices of the U. S. Atomic Energy Commission.

† Now at the Department of Physics, George Washington University, Washington, D. C.

¹ Cowan, Reines, Harrison, Kruse, and McGuire, *Science* **124**, 103 (1956).

² Ronzio, Cowan, and Reines, *Rev. Sci. Instr.* **29**, 146 (1958), describe the preparation and handling of liquid scintillators developed for the Los Alamos neutrino program.

³ F. Reines and C. L. Cowan, Jr., *Phys. Rev.* **90**, 492 (1953).

⁴ The gain, times 6.5, due to the increase in target protons was largely balanced by a decrease in the neutron detection efficiency, times $\frac{1}{3}$, made necessary by other experimental considerations.

II. THE EXPERIMENT

Figure 1 represents schematically the sequence of events which occur when an antineutrino is captured by a proton. The cross section $\bar{\sigma}$ for the process for an average fission $\bar{\nu}$ is determined from the relation

$$\bar{\sigma} = \frac{R}{3600fn\epsilon_{\beta^+}\epsilon_n} \text{ cm}^2, \quad (2)$$

where R = the observed signal rate in counts/hr; n = the number of target protons = 8.3×10^{28} ; f = the antineutrino flux at the detector in $\bar{\nu}/\text{cm}^2 \text{ sec} = 1.3 \times 10^{13}$, assuming $N = 6.1$ $\bar{\nu}$ /fission; ϵ_{β^+} = the positron detection efficiency, and ϵ_n = the neutron detection efficiency.

Note that the mean cross section per fission ($N\bar{\sigma}$) is independent of the number of antineutrinos assumed emitted by the fission-fragments per fission (N). Uncertainties in the $\bar{\nu}$ flux f (5 to 10%) arise from imprecise knowledge of reactor power, uncertainty concerning energy released per fission and the number of $\bar{\nu}$ per fission, and incomplete knowledge of the fission-fragment distribution in the reactor. The $\bar{\nu}$ energy spectrum is determined from a measured β^+ spectrum (or the first-pulse spectrum of the antineutrino-produced delayed coincidences after appropriate energy-resolution corrections). The energy $E_{\bar{\nu}}$ of the $\bar{\nu}$ is related to E_{β^+} , the kinetic energy of the product β^+ , by the equation

$$E_{\bar{\nu}} = 3.53 + E_{\beta^+} (mc^2 \text{ units}). \quad (3)$$

We have neglected the few-kilovolt recoil energy of the product neutron.

With these quantities in mind we will describe the experiment in conjunction with a schematic diagram of the equipment (Fig. 2).⁵ Assume that an antineutrino-

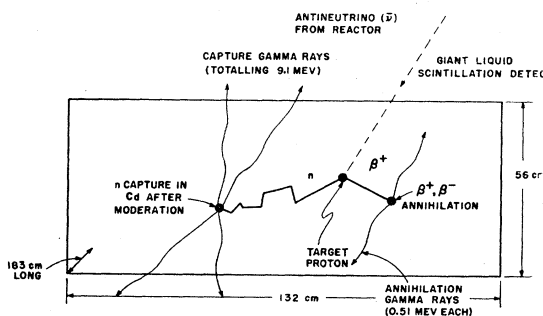


FIG. 1. Schematic of antineutrino detector. This 1.4×10^3 -liter detector is filled with a mixture which consists primarily of triethylbenzene (TEB) with small amounts of *p*-terphenyl (3 g/liter), POPOP wavelength shifter (0.2 g/liter) and cadmium (1.8 g/liter) as cadmium octoate. An antineutrino is shown transmuting a proton to produce a neutron and positron. The positron slows down and annihilates, producing annihilation radiation. The neutron is moderated by the hydrogen of the scintillator and is captured by the cadmium, producing capture gamma rays.

⁵ Photographs of the detectors and some associated equipment may be found in F. Reines and C. L. Cowan, Jr., *Physics Today* 10, No. 8, 12 (1957). Detector details are described in an article

induced reaction occurs in the detector. The β^+ signal is seen by each of two interleaved banks of 55, 5-inch Dumont photomultiplier tubes in prompt coincidence within the 0.2- μsec resolving time of the equipment. The signals are added by preamplifiers whose gains have been balanced to allow for slight differences in the response of the two photomultiplier banks, amplified further and sent via a 30- μsec delay line to the deflection plates of a recording oscilloscope. At the same time the two signals are sent separately to a prompt coincidence unit (marked β^+) which accepts them if they correspond to pulse-height amplitudes between 1.5 and 8 Mev. On receipt of an acceptable signal, the β^+ scaler is tripped, and a gating pulse is sent to the second coincidence unit (marked n). If during a prescribed time (0.75 to 25.75 μsec) following the β^+ pulse, a neutron pulse corresponding to an energy deposition of 3 to 10 Mev in the antineutrino detector occurs (again in prompt coincidence from the two interleaved photomultiplier banks), the neutron coincidence unit signals a delayed coincidence. This delayed coincidence is registered by a scaler and triggers the scope sweep, allowing the entire sequence which has been stored in in the 30- μsec delay lines to be displayed and photographed. The neutron prompt coincidences are also recorded by a scaler.⁶ Therefore the raw data obtained for analysis are the following: the rates in the positron and neutron gates, delayed coincidence rate, scope trigger rate, pulse amplitudes, and time intervals between pulses as seen on the recording oscilloscope. These data are obtained with the reactor on and off and with gross changes in bulk shielding provided by bags of wet sawdust.

In addition to the above arrangement there is provision for the reduction of cosmic-ray-associated background by means of an anticoincidence detector placed above the antineutrino detector as shown in Fig. 2. If, for example, a pulse occurs in the anticoincidence detector of amplitude >0.5 Mev in coincidence with otherwise acceptable β^+ -like pulses, the event is not accepted by the β^+ coincidence-anticoincidence unit and hence is not recorded by the oscilloscope. This is a reasonable criterion since the annihilation radiation which might reach the anticoincidence detector for a bonafide $\bar{\nu}$ event is at most 0.5 Mev. In order to reduce the background from events secondary to the passage of high-energy (>8 Mev) charged cosmic rays and delayed in time, the β^+ coincidence unit had incorporated into it a long gate which rendered the system insensitive for ~ 60 μsec following such a pulse. Pulses triggered by electrical noise are also eliminated by means of the distinctive visual record.

by F. Reines in the forthcoming book, *Methods of Experimental Physics*, edited by L. C. Yuan and C. S. Wu [Academic Press, Inc., New York (to be published)], Vol. 5.

⁶ To be precise, we should use the phrases " β^+ -like" and " n -like" to describe the pulses because pulses in these energy ranges are produced by other particles as well.

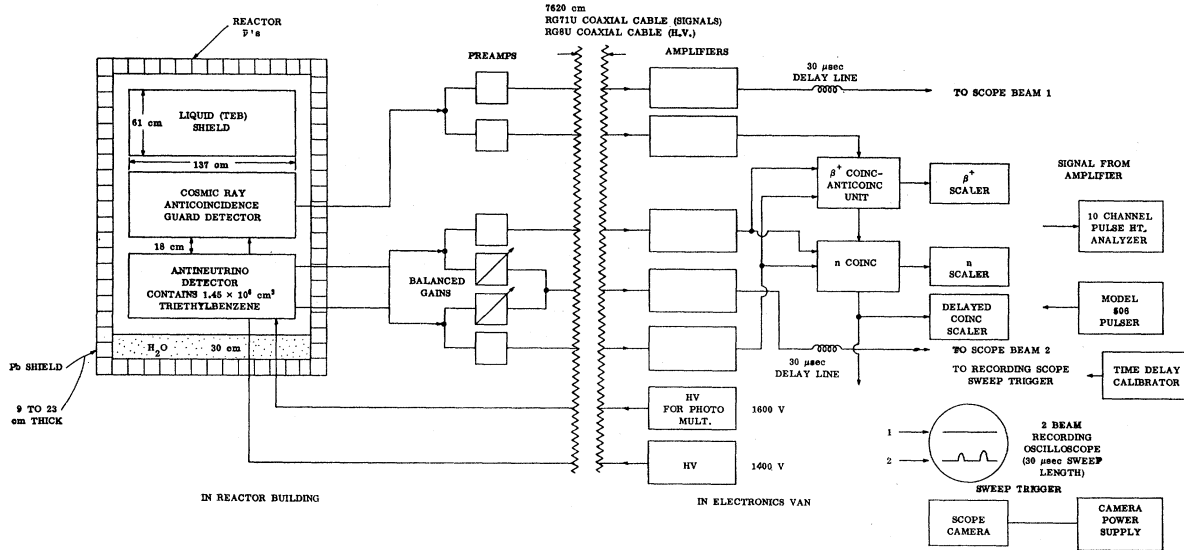


Fig. 2. Schematic of experimental arrangement.

A. Calibration

Calibrations of energy and time-interval response were made periodically. The first was accomplished by employing the μ -meson "through-peak" energy, the second by means of standard time markers put directly on the oscilloscope traces by a crystal oscillator. Gate lengths were checked against a time-delay calibrator designed for the purpose. Figure 3 shows the through-peak, a pulse-amplitude distribution resulting from the vertical passage through the tank of penetrating cosmic-ray μ mesons, taken before and after the present experiment for each of the two interleaved photo-multiplier tube banks. Since most of the mesons are minimally ionizing, and the depth of the liquid is 60 cm, the specific energy loss⁷ in the liquid of 1.57 Mev/cm gives the location of the peak as 100 Mev. The peak represents a slightly higher energy than that calculated from the energy loss/cm times the tank depth because of the finite lateral extent of the tank and the angular distribution of the cosmic rays. The peak is located to an accuracy of $\pm 5\%$. Since the detector response is proportional to the energy deposited in it, a standard linear pulser was calibrated with the through-peak amplitude and then used to calibrate the system in turn and set the appropriate gates. Based on measurements using artificial radioactive sources and the end point of the electron spectrum from μ -meson decay in our large liquid scintillation detectors, the error in energy calibration is believed to be less than $\pm 10\%$.

B. Determination of the Signal Rate R

The signal rate R was determined from the four series of measurements summarized in Table I. In

⁷ This value is obtained from Fig. 2.91 of the book by B. Rossi, *High-Energy Particles* (Prentice-Hall, Inc., Englewood Cliffs, New Jersey, 1952), using a carbon density of 0.88 g/cm³.

principle the procedure is straightforward: the accidental background rate A (hr^{-1}) is determined for each run from the relation

$$A = 3600\alpha\bar{n}\bar{\beta}^+\tau \text{ hr}^{-1}, \quad (4)$$

where τ = delayed-coincidence gate length in sec = 25×10^{-6} ; α = overlap factor for counts in n and β^+ gates; \bar{n} and $\bar{\beta}^+$ = the rates in the neutron and positron gates averaged over each run as measured by the scalars.

We see from a comparison of the delayed-coincidence rate as given by the scalars and film analysis, however, that about $\frac{1}{3}$ of the scaler rate is rejected as unsuitable on inspection of the film traces. This means that the accidental background rate calculated from the n and β^+ scalars is too high by a factor of about $\frac{1}{3}$. In addition, the energies in the n and β^+ gates

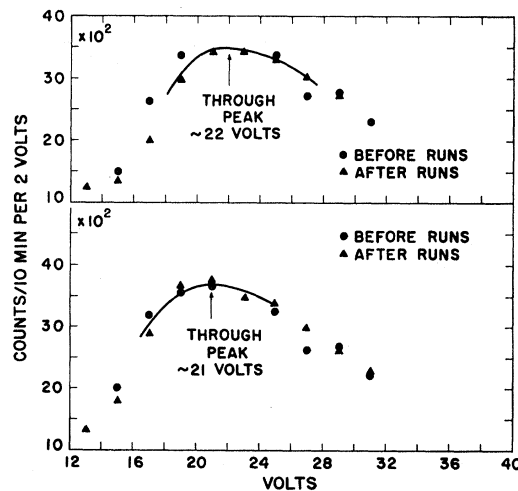


Fig. 3. Ungated meson through-peaks for energy calibration and stability check.

TABLE I. Summary of runs (a).

Run No. ^a	Comments	Run length (hr)	$n(\text{sec}^{-1})$	Scaler readings		Total scope film accept. rate (hr^{-1}) (in 25 μsec)
				$\bar{\beta}^+(\text{sec}^{-1})$	Del. coinc (hr^{-1}) (25 μsec gate)	
232	Reactor <i>ON</i> , wet saw- dust shield in place. (Category <i>A</i>)	2.05	15.9	68.5	307.8	212.6
233		14.43	15.8	67.5	304.5	220.3
234		8.0	15.6	66.6	302.6	209.4
235		13.30	15.6	66.8	297.8	205.3
236		9.5	15.4	67.0	299.5	214.8
237	Reactor <i>OFF</i> , sawdust shield in place. (Category <i>B</i>)	12.47	14.3	65.0	251.0	165.6
238		9.37	14.0	63.6	249.0	170.9
240		9.54	14.2	68.0	256.6	173.7
241		14.43	14.5	66.3	251.8	170.1
243		6.77	14.4	65.4	251.1	163.5
246	Reactor <i>ON</i> , sawdust shield in place. (Category <i>C</i>)	12.20	16.3	71.6	313.4	228.3
247		2.00	16.2	71.1	300.0	213.5
248		11.12	16.1	71.1	314.5	224.4
249		9.53	16.2	71.2	327.2	236.6
251		10.53	16.5	72.4	320.9	226.2
252		11.67	16.2	71.5	324.7	232.6
253		8.92	16.3	71.6	316.3	222.5
255	Reactor <i>ON</i> , sawdust removed. (Category <i>D</i>)	6.48	17.2	75.2	334.4	250.5
256		10.38	17.3	76.0	331.1	240.2

^a Runs are listed in chronological sequence. Missing runs were omitted either because they were incomplete or were not a relevant part of this series.

overlap, and judging by the rates in these gates, $1.23 > \alpha > 1.00$. Basing our calculations on the scope films, we find the net rates (total less accidental) for the four categories of runs which we list in Table II. Since $\alpha < 1.23$ and the truth is between (a) and (c), we quote $R = 36 \pm 4 \text{ hr}^{-1}$, where ± 4 includes the statistical error listed in column (a) and an allowance for the drift in the energy calibration, which analysis of the data shows likely to have occurred in the period between the series of runs *A* and *C*. The ratio of the n/β^+ rates is lower for runs *C* than for *A*. This is consistent with an increase in the over-all gain of the system, since the background spectrum decreases monotonically with increasing energy, and an increase in gain would bring in relatively more low-energy pulses. Runs *D* were made to demonstrate that the sawdust shield, though effective in reducing neutron signals from an Am-Be source (and hence reactor neutrons) by a factor of 15 and gammas by a factor of 2, had no effect on the antineutrino signal. The antineutrino flux during *D* was up by 10% because of a

change in reactor power which happened to coincide with these runs. When corrected for this rise in reactor power, the results from *D* are consistent with the other runs.

C. Signal-to-Background Ratio

From Tables I and II we conclude that the signal-to-total-background ratio is approximately $\frac{1}{5}$, with the background about equally divided between correlated and accidental events. Correlated events arise primarily from fast neutrons produced by μ -meson capture in the vicinity of the detector: the first pulse is produced as a proton recoil, the second by the capture of the neutron in the scintillator cadmium. The correlated reactor-associated background is deduced from the absence of an observable effect due to the 75-cm sawdust shield (density, 0.5 g/cm³; neutron shielding factor, 15) to be $< 1/10$ the signal. An accidental background increase of 15 hr^{-1} was associated with the reactor so that the ratio of signal to accidental reactor-associated background was about 2/1.

TABLE II. Summary of results (b).

Run category	Net rate (hr^{-1}) = Gross rate less calculated accidental background			Results Reactor associated signal = $[(C-B)66 + (A-B)47.3]/113.3$
	(a) Bkd. reduced by signal ratio and $\alpha = 1$	(b) No correction "1/3" factor and $\alpha = 1$	(c) Correction "1/3" factor and $\alpha = 1$	
<i>A</i> (47.3 hr)	146.2 \pm 1.7	118.4	130.8	(a) 38 \pm 3 (hr^{-1})
<i>B</i> (52.6 hr)	112.2 \pm 1.5	84.4	99.1	(b) 37 \pm 3
<i>C</i> (66.0 hr)	153.0 \pm 1.4	123.3	135.8	(c) 35 \pm 3
<i>D</i> (16.9 hr)	157.9 \pm 2	126.6	138.1	

D. Efficiency Estimates

In order to evaluate the cross section, we require the efficiencies ϵ_{β^+} and ϵ_n . Since these quantities were inferred rather than measured directly, some discussion of the efficiency evaluation procedure employed is in order.

$$\epsilon_{\beta^+}$$

It is evident that the β^+ -detection efficiency is high because of the small probability of β^+ leakage from the detector. The problem is to determine the probability that an event will fall within the energy gates employed, i.e., 1.5 to 8 Mev. To estimate this probability, plots were made of the first-pulse spectrum with the reactor on and off as measured in runs A, B, and C. Figure 4 shows the spectrum of first pulses scaled to run time of 47.3 hr. The lowest energy points are seen to drop sharply, a fact attributed to the effect of energy gates cutting into the spectrum. Since the background spectrum should continue to rise with decreasing energy,

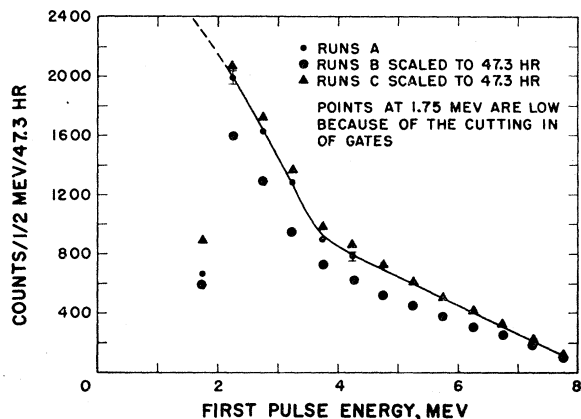


FIG. 4. First-pulse spectrum.

the reactor on-off difference was scaled up by a factor determined from an extrapolation to lower energies and is shown on the first-pulse difference curve on Fig. 5. In deriving the difference curve, no account was taken of the increase in accidental background associated with the reactor, and so the curve rises more sharply at lower energies than does the true β^+ spectrum. The β^+ detection efficiency was deduced from this curve by extrapolating to the origin and measuring the fraction of the area in the experimental *vs* the extrapolated curve. This procedure underestimates the efficiency somewhat because a subsequent measurement of the ungated spectrum seen from a Cu^{64} β^+ source dissolved in the scintillator showed no pulses of energy < 0.45 Mev, whereas we have here assumed pulses down to 0 Mev. Accordingly, the β^+ efficiency estimate from Fig. 5 (0.81) is raised slightly and taken to be $\epsilon_{\beta^+} = 0.85 \pm 0.05$, where 0.05 is meant to indicate the limits of error in ϵ_{β^+} .

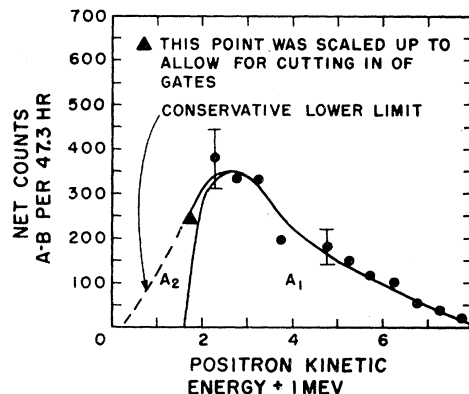


FIG. 5. Positron spectrum, $A_1/(A_1+A_2)=0.81$. No correction is made here for reactor-associated background. This background raises the lower-energy part of the spectrum and hence $\epsilon_{\beta^+} > 0.81$. Take $\epsilon_{\beta^+} = 0.85 \pm 0.05$.

$$\epsilon_n$$

The neutron-detection efficiency is somewhat more difficult to estimate. This efficiency is given as the product of three factors:

$$\epsilon_n = \epsilon_{n1}\epsilon_{n2}\epsilon_{n3}, \tag{5}$$

where ϵ_{n1} =probability that the neutron will not leak out of the system, ϵ_{n2} =probability that the neutron will be captured in the scintillator cadmium in the 25- μ sec time interval (0.75 to 25.75 μ sec) after its birth, and ϵ_{n3} =probability that the neutron capture gamma rays will produce a signal which falls within the chosen energy gates, 3 to 10 Mev.

We estimate ϵ_{n1} from a consideration of the detector-volume fraction within an antineutrino-produced neutron mean free path of the detector surface. From the conservation laws applied to reaction (1) the neutron energy is $\lesssim 10$ keV and therefore has a mean free path in the scintillator of about 1 cm. The fraction of the detector volume within 1 cm of the edge is about 6% and approximately $\frac{1}{2}$ (or 3%) of the neutrons born in this region will be travelling outward; hence $\epsilon_{n1} = 0.97$.

The least certain of the factors involved in the neutron-detection efficiency is ϵ_{n2} . It was estimated in

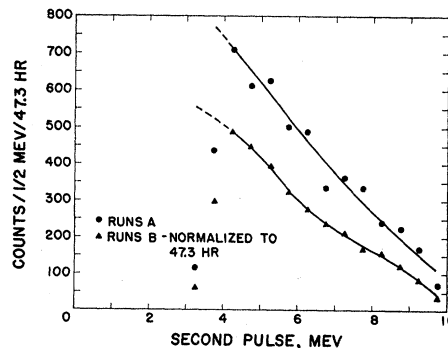


FIG. 6. Second-pulse spectrum.

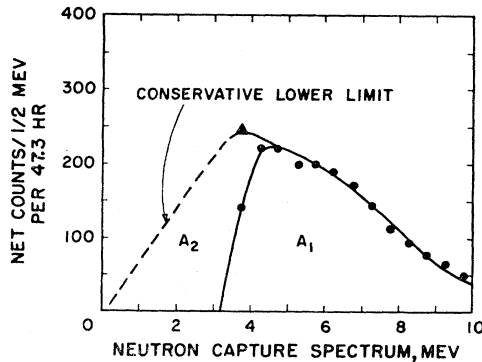


FIG. 7. Neutron-capture gamma spectrum. $A_1/(A_1+A_2)=0.68$. No correction is made here for reactor-associated background. This background raises the lower-energy part of the spectrum and hence $\epsilon_{n_3} > 0.68$. Take $\epsilon_{n_3} = 0.75 \pm 0.05$.

two ways: by an interpolation of the curves calculated via the Monte Carlo method for cases⁸ involving higher Cd/H ratios than the one used in this experiment (here Cd/H=0.000145) and by integration of the cadmium-capture probability for thermal neutrons from 0.75 to 25.75 μsec after their introduction into the scintillator. The interpolation gives $\tau_{n_2} = 0.15$ with a ± 0.02 uncertainty. If capture competition by the scintillator hydrogen is neglected, the mean time for capture $\tau_{\text{Cd}} = 161 \mu\text{sec}$, and the capture probability is

$$\bar{\sigma} = \frac{36 \pm 4}{3600 \times 1.3 \times 10^{13} \times 8.3 \times 10^{28} \times (0.85 \pm 0.05) \times (0.10 \pm 0.02)} = 11 \pm 2.6 \times 10^{-44} \text{ cm}^2/\bar{\nu},$$

or

$$N\bar{\sigma} = 6.7 \pm 1.5 \times 10^{-43} \text{ cm}^2/\text{fission},$$

where we have quoted the root-mean-square error.

This value of the cross section is consistent with

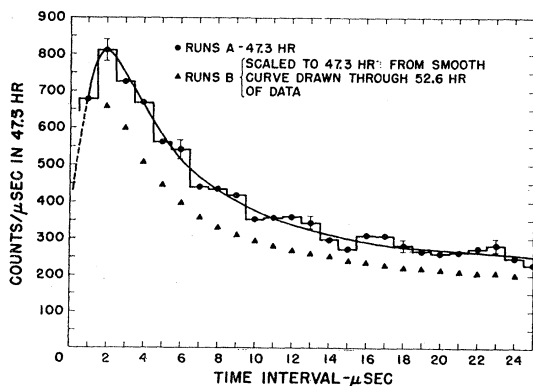


FIG. 8. Distribution of time intervals between pulses. ● Runs A (47.3 hr). ▲ Runs B (scaled to 47.3 hr from smooth curve drawn through 52.6 hr of data).

⁸ Reines, Cowan, Harrison, and Carter, Rev. Sci. Instr. 25, 1061 (1954).

calculated to be 0.142. Since the mean capture time in scintillator hydrogen $\tau_{\text{H}} = 235 \mu\text{sec}$, the hydrogen captures in this period reduce the number of captures in Cd so that $\epsilon_{n_2} = 0.135$.

We estimated ϵ_{n_3} in much the same way as ϵ_{β^+} . Figure 6 shows the first-pulse spectra in runs A and B normalized to 47.3 hr. Figure 7 shows the difference spectrum and $A_1/(A_1+A_2) = 0.68$. Since, as with the first-pulse spectrum, no allowance was made for the accidental background, we take

$$\epsilon_{n_3} = 0.75 \pm 0.05,$$

where ± 0.05 is meant to indicate the limits of error in ϵ_{n_3} .

To summarize, $\epsilon_n = 0.97 \times 0.75 \times 0.14 = 0.10$. It seems reasonable to assign error limits of $\pm 20\%$ to this efficiency. An experimental attempt to measure the neutron-detection efficiency succeeded only in setting a lower limit of 6%. Figures 8 and 9 show the distribution of time-delay intervals between the pairs of pulses comprising the delayed coincidences. The curves are characteristic of neutron captures in the scintillator.⁸

E. The Cross Section

Inserting the efficiency numbers, etc., into Eq. (2) we find the cross section for fission antineutrino absorption by protons:

predictions based on the two-component theory of the neutrino.⁹

F. The $\bar{\nu}$ Spectrum from Fission Fragments

It is possible to deduce the fission fragment $\bar{\nu}$ spectrum from a measurement of the β^+ energies in reaction (1) and a knowledge of the cross section for the process. Because of the large experimental error involved in our determination of the β^+ spectra, the resultant $\bar{\nu}$ spectrum is very poorly determined. Nonetheless it seems worthwhile to make such a deduction. Apart from statistical fluctuations, the major uncertainty is in the energy resolution of the system. This uncertainty is due to leakage of one 0.511-Mev annihilation gamma ray from the detector and the poor energy resolution ($\pm 25\%$) for 1 Mev deposited in the large detector. The effect of gamma-ray leakage on the spectrum was checked by dissolving a Cu^{64} -octoate source in the scintillator and measuring the energy

⁹ The cross sections for monoenergetic $\bar{\nu}$ and for the measured $\bar{\nu}$ spectrum for fission fragments are given by Carter, Reines, Wagner, and Wyman, Phys. Rev. 113, 280 (1959), following paper.

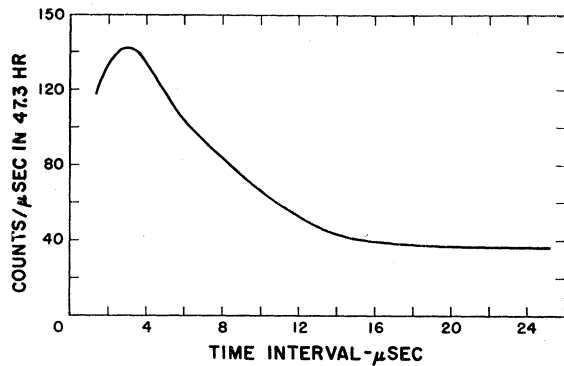


FIG. 9. Reactor-associated distribution of time intervals between pulses. Runs A-B (normalized to 47.3 hr).

spectrum. It was somewhat distorted, but the main effect was to drop the energy by about 0.5 Mev.

The β^+ spectrum $n(E_{\beta^+})$, the cross section for monoenergetic $\bar{\nu}$, $\sigma(E_{\bar{\nu}})$ and the $\bar{\nu}$ spectrum $m(E_{\bar{\nu}})$ are related⁹ by the equation

$$m(E_{\bar{\nu}}) = n(E_{\beta^+}) / \sigma(E_{\bar{\nu}}). \quad (6)$$

Figure 10 shows $m(E_{\bar{\nu}})$. Gamma-ray leakage was considered in that the β^+ curve was shifted to the right by 0.5 Mev prior to the calculation. The data are not considered sufficiently accurate to warrant estimation of the distortion due to the energy resolution of the detector.

III. REMARKS CONCERNING AN IMPROVED MEASUREMENT

At least two major improvements could be made in this measurement to increase the counting rate and improve the energy resolution. The neutron-detection efficiency can be raised from its present 10% to about 80% by increasing the cadmium content of the scintillator by a factor of 20. This can be done without unreasonable reduction in the light transmission and scintillator efficiency by using the highly purified cadmium octoate recently developed by Ronzio.¹⁰

In addition, redesign of the detector using an inner "cadmiated" region enclosed in a noncadmium-bearing scintillator would minimize end effects due to gamma-ray leakage from the detector. Such an increase in detection efficiency would permit a factor of ten reduction in the size of the antineutrino-sensitive (or

¹⁰ A. R. Ronzio (private communication). Another solution, cadmium propionate in toluene with the suggested Cd/H ratio of 0.003, was used in the Hanford work^{3,8} but its generally undesirable characteristics, e.g., fire hazard and toxicity, militated against its use in the present experiment.

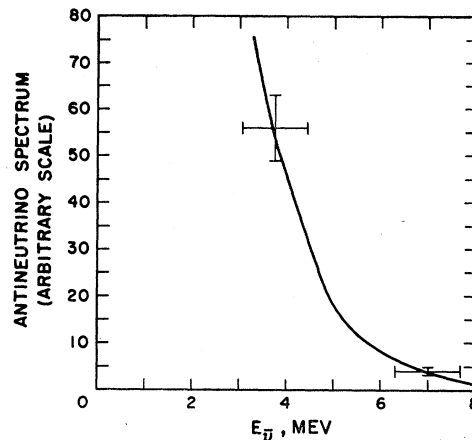


FIG. 10. Antineutrino spectrum from fission fragments deduced from β^+ spectrum in reaction $\bar{\nu}(p^+, n)\beta^+$. Crosses denote estimates of uncertainties.

cadmiated) volume without undue sacrifice in signal rate. At presently available antineutrino fluxes, a signal rate of 30 hr⁻¹ or more would result from the smaller improved detector. The signal-to-accidental-background ratio would be raised by a factor of about ten for a 25- μ sec delayed-coincidence gate because of the increase in the signal rate and the decrease in detector size. The uncadmiated scintillator blanket should help shield against cosmic-ray-correlated events which are due to a neutron produced by μ -meson capture in the vicinity of the detector. A cylindrical shape with photomultiplier tubes placed around the cylinder wall would make for a uniform light collection and hence improved energy resolution. This detector could be shielded against cosmic rays with the anti-coincidence detector as before, and much the same electronics could be used.

IV. ACKNOWLEDGMENTS

The authors wish to thank Mr. H. W. Kruse for his analysis of the film records. Dr. F. B. Harrison and Dr. A. D. McGuire and R. P. Jones and M. P. Warren helped set up the equipment. Many groups in the Los Alamos Scientific Laboratory have given support in the design and construction of the equipment. We wish especially to thank the Shops Department under Mr. G. H. Schultz and the Electronics Group under Mr. John Lamb. The hospitality of the E. I. duPont de Nemours Company, which operates the Savannah River Plant of the United States Atomic Energy Commission, is also gratefully acknowledged.